

## Competition of Multiple Spin Exchanges in Submonolayer Solid $^3\text{He}$

Hiroki Ikegami, Ken Obara, Daisuke Ito, and Hidehiko Ishimoto

*Institute for Solid State Physics, University of Tokyo, 7-22-1 Roppongi, Minato-ku, Tokyo 106-8666, Japan*

(Received 6 May 1998)

We have made NMR measurements of the first layer of solid  $^3\text{He}$  adsorbed on graphite down to  $120\ \mu\text{K}$ . Magnetization varies from antiferro- to ferromagnetic on increasing the coverage except for the region around the  $\sqrt{3} \times \sqrt{3}$  commensurate phase. This behavior is very similar to that of the second layer and is understood as due to the competition among various multiple spin exchanges. The  $\sqrt{3} \times \sqrt{3}$  phase exhibits a ferromagnetic behavior which is not expected from a simple coverage dependence of the multiple exchange energies. [S0031-9007(98)07102-6]

PACS numbers: 67.80.Jd, 67.70.+n, 75.70.Ak

Multiple spin exchange (MSE) is of great importance in understanding the magnetic properties of solid  $^3\text{He}$  [1]. In this quantum solid, the higher order cyclic exchanges such as three- or four-particle exchange are favored over the simple interchange of two atoms, because of a strong hard core repulsive potential between atoms. Exchange of an even number of particles is antiferromagnetic (AFM), while that of an odd number is ferromagnetic (FM). The existence of two competing interactions makes the system intrinsically frustrated, leading to various peculiar magnetic properties both in bulk and in adsorbed  $^3\text{He}$  [2].

Recent studies of solid  $^3\text{He}$  films adsorbed on graphite have proved to provide a truly two-dimensional frustrated  $S = 1/2$  quantum spin system. Especially in the second layer, the magnetic properties change dramatically with the coverage [3]. At the density just solidified from the fluid phase, the exchange interaction is antiferromagnetic. On increasing the coverage and the third layer's promotion, the magnetization shows a crossover from AFM to FM, followed by a large ferromagnetic peak. This magnetic behavior is qualitatively explained by the MSE model [4]. However, the existence of the third layer fluid allows a Ruderman-Kittel-Kasuya-Yosida type indirect exchange process which could also explain the ferromagnetism in the second layer [5–7]. It is not yet clearly understood until now whether the liquid overlayer has an active role for the spin interaction of the second layer.

On the other hand, the first layer completely solidifies into a registered  $\sqrt{3} \times \sqrt{3}$  commensurate ( $R$ ) phase at  $6.4\ \text{nm}^{-2}$ , and the second layer promotion does not occur until about  $11\ \text{nm}^{-2}$  due to a stronger adsorption potential. So the monolayer system is compressed by about 40% before the second layer promotion. This is a great advantage since we can investigate the effect of MSE for a wide range of density without the influence of the liquid overlayer. However, the nuclear exchange energy is an order of magnitude smaller than that of the second layer, and therefore measurement should be done at temperatures well below 1 mK.

In this Letter we present new extensive NMR measurements of the first layer solid  $^3\text{He}$  adsorbed on graphite

down to  $120\ \mu\text{K}$ , much lower than the previous [8,9]. On increasing the coverage, the magnetization evolves with some specific features which are similar to those observed in the second layer except for the  $\sqrt{3} \times \sqrt{3}$  phase where a ferromagnetic behavior is found.

The substrate used in this work is exfoliated graphite (Grafoil GTY grade 76  $\mu\text{m}$  thick) with a surface area of  $11.4\ \text{m}^2$  [10]. Two Grafoil sheets were diffusion bonded on either side of a silver foil 20  $\mu\text{m}$  in thickness. Tabs extending from a total of 42 silver foils were also diffusion bonded to a silver rod to ensure good thermal contact. The rod was tightly connected to a powerful copper nuclear demagnetization stage [11]. The time constant for thermal equilibrium was typically 20 min even at  $180\ \mu\text{K}$ , and no hysteresis was observed in magnetization on cooling and warming, indicating good thermal contact. The temperature was determined by a platinum pulsed NMR thermometer calibrated against a  $^3\text{He}$  melting curve or the superfluid transition of liquid  $^3\text{He}$ . Samples were prepared by admitting a known amount of  $^3\text{He}$  gas into the epoxy covered sample cell at temperature above 4 K. After being annealed above 8 K overnight, they were cooled down very slowly. NMR measurements were made by a continuous wave method at a frequency of 623 kHz corresponding to a static field of 19.2 mT parallel to the graphite plane. The field was swept to cover the whole NMR line, usually 6 to 12 times for averaging. Magnetization ( $M$ ) was obtained from a numerical integration of the absorption line. The uncertainty of  $M$  is of the order of 3% at 1 mK, which is mainly due to the uncertainty of subtraction of the base line.

We have measured 14 coverages ranging from 5.0 to  $8.5\ \text{nm}^{-2}$ . All data including the coexisting region with liquid exhibit the Curie-Weiss behavior. The typical results are shown in Fig. 1, where the data are plotted as  $M$  times temperature  $T$  against  $T$  to emphasize the deviations from the Curie law. Apparent deviation from the Curie law is seen at temperatures below 1 mK, exhibiting a strong coverage dependence.

Figure 2(a) shows the evolution of  $MT$  at several temperatures as a function of areal density. Here the dashed

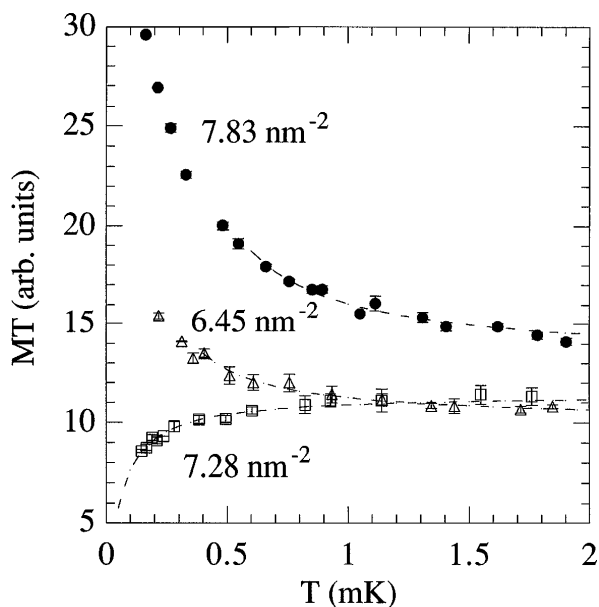


FIG. 1. Typical magnetization results where the products of the magnetization and temperature are plotted as a function of temperature. Dashed lines are those fitted to the Curie-Weiss law.

line corresponds to a free spin behavior. To help the understanding of the present results, the heat capacity isotherm at 2.5 mK [12], where the nuclear spin contribution is dominant, is shown in Fig. 2(b). Here to compare with the heat capacity data, the areal density is determined such that a cusplike maximum in the NMR absorption linewidth for the second layer promotion corresponds to  $11.2 \text{ nm}^{-2}$ , the value estimated by Greywall and Busch from the heat capacity [12,13]. This coverage scale is only 1.0% higher than the other scale in which the high density end of the substep in our vapor pressure isotherm of adsorbed  $\text{N}_2$  at 77 K corresponds to  $6.4 \text{ nm}^{-2}$ .

With increasing coverage the magnetization behaves in a very interesting way. After enhancement of  $M$  from the free spin value at the  $R$  phase, it has changed to AFM behavior for  $7.07 \text{ nm}^{-2}$ . Then the magnetization is found FM again at  $7.41 \text{ nm}^{-2}$ , followed by a large ferromagnetic peak at around  $7.6 \text{ nm}^{-2}$ . This behavior is very similar to that of the heat capacity isotherm, including some special densities which correspond to the changes in structural or magnetic properties. All coverage data can be well fitted by the Curie-Weiss law  $M = C/(T - \theta)$ , as long as the spin polarization is not so large (dashed lines in Fig. 1). The Curie constant  $C$  for the coverages below  $7.41 \text{ nm}^{-2}$  is found to be systematically 5% smaller than expected as pointed out in Ref. [9]. The fitting at  $7.83 \text{ nm}^{-2}$  down to  $600 \mu\text{K}$  gives an effective exchange energy  $J_\chi = \theta/3 = 59 \pm 7 \mu\text{K}$ . We also tried to fit the data to the 10 terms high temperature series expansion for a ferromagnetic Heisenberg model in two dimensional triangular lattice. The fitting in a little bit wider temperature range down to  $0.45 \text{ mK}$  gives

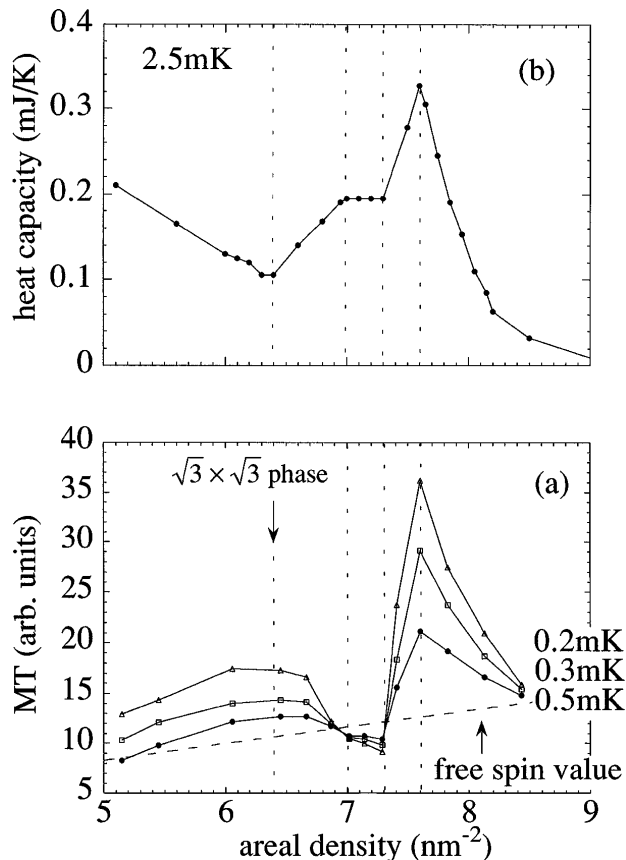


FIG. 2. (a) The products of magnetization and temperature isotherms as a function of coverage. Dashed line is for the free spin behavior. (b) The heat capacity isotherm at 2.5 mK from Ref. [12].

us  $J_\chi = 63 \mu\text{K}$ , which agrees with that from the Curie-Weiss fitting within an error bar. The data at  $7.28 \text{ nm}^{-2}$  are well fitted over the whole temperature range down to  $150 \mu\text{K}$ , leading  $J_\chi = -16 \pm 3 \mu\text{K}$ . The obtained  $J_\chi$  is shown in Fig. 3 as a function of areal density.

The most important feature is the existence of both AFM and FM regions at the high density side. This behavior is analogous to that in the second layer where MSE processes play an important role. Since the interactions in the first layer are generated only by in-plane exchange processes, they can be calculated from first principles by path integral Monte Carlo techniques. Nevertheless, calculations have been carried out mostly at a single density [14]. To discuss the density dependence, the various  $n$ -particle exchange energies  $J_n$  are estimated within a WKB approximation developed by Roger [4]. In this approximation, especially the two-particle exchange has a stronger density dependence than the other ones. At high density a three-particle exchange is dominant, causing a ferromagnetic behavior there. While at low density a two-particle exchange is comparable with the three-particle exchange, changing an effective interaction from FM to AFM with decreasing the areal density. The effective exchange energy is given as  $J_\chi = -(J_2 - 2J_3 + 3J_4 + 5/8J_6)$

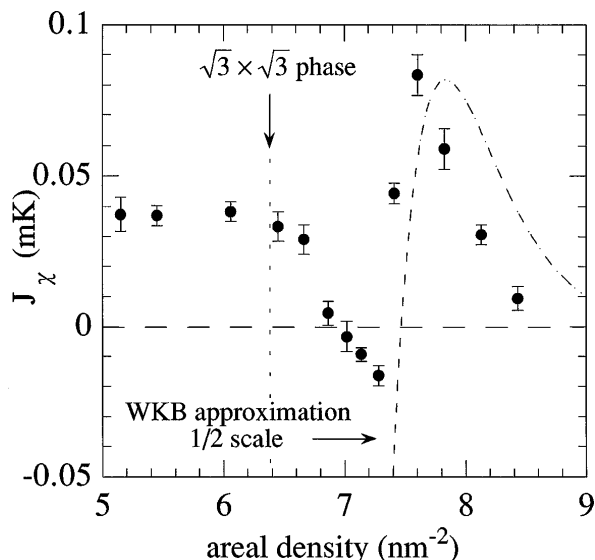


FIG. 3. Effective exchange energy as a function of the coverage. Dashed line is the effective exchange energy calculated within a WKB approximation in Ref. [4].

and is calculated using the parameters in Ref. [4] as shown in Fig. 3. The calculated density dependence qualitatively reproduces our data above  $7.3 \text{ nm}^{-2}$  except for the absolute value and the small shift of density.

In the incommensurate (IC) phase above  $7.6 \text{ nm}^{-2}$ ,  $J_\chi$  is different from the effective exchange constant ( $J_c$ ) obtained from a heat capacity measurement [15] or  $J$  from a relaxation time of NMR performed at 1 K [16].  $J_\chi$  is about a factor of 3 smaller than  $J_c$  and an order of magnitude smaller than  $J$  at the same density. This discrepancy is consistent with the MSE model: multiple spin exchange enhances the nuclear relaxation but a strong cancellation occurs in the effective exchange energy  $J_\chi$ .  $J_c$  comes just in between. Thus  $J_4$  and  $J_6$  are not negligible and the competition between AFM and FM interaction still remains even in the FM region.

Both  $M$  and the heat capacity above  $7.0 \text{ nm}^{-2}$  exhibit a very similar evolution to those in the second layer [15,17]. That is, at low density corresponding to the AFM behavior, the heat capacity shows a plateau and is followed by a large peak at almost the same density with a magnetization peak. This fact implies that both layers evolve in a similar way in the structural and magnetic properties. Therefore the mechanism giving rise to the FM interaction in the second layer could also be the in-plane exchange process, and the overlaying liquid would not play an important role.

This analogy between both layers gives other information on the structure. In the second layer the AFM commensurate phase rearranges to the FM incommensurate across the transitional region where the coexistence between both phases is not yet clear [18,19]. The same seems to occur between  $7.3$  and  $7.6 \text{ nm}^{-2}$  in the first

layer although the transition region is very narrow. If so, the lower density phase could be a stable commensurate phase which exists at around  $7.3 \text{ nm}^{-2}$ . The higher density incommensurate phase should begin at  $7.6 \text{ nm}^{-2}$ . In the same density region Greywall and Busch proposed a slightly different structure where their commensurate phase  $R_{1b}$  coexists with the incommensurate phase up to  $8.1 \text{ nm}^{-2}$  [12]. This proposal is not consistent with the present magnetization isotherm. If two phases with different magnetic properties coexist, the magnetization peak should come not in the transitional region but at the boundary of the coexistence region.

The other striking feature is the FM behavior before complete solidification at  $6.4 \text{ nm}^{-2}$ .  $J_\chi$  is almost constant there, indicating that the solid phase is the  $\sqrt{3} \times \sqrt{3}$  phase although it coexists with the liquid. Such a ferromagnetic behavior at the  $R$  phase is not expected from a simple density dependence of the multiple exchange energies as mentioned above. Actually AFM behavior is found at about the same density in the second layer and the stronger AFM behavior is observed at the lower density in the submonolayer  $^3\text{He}$  system adsorbed on two layers of HD [20]. In the first layer one cannot neglect a corrugation potential from the substrate structure along the surface, since the  $R$  phase is stabilized by it. The potential is an order of 40 K deeper at the center of the graphite hexagons than at its corner or side [21]. In the exchange process, the tunneling atoms should keep away from the barrier of the corrugation potential as well as from the hard core potential of the surrounding atoms. This should cause the reduction of the exchange frequency. The effect from the substrate potential would be different for each  $n$ -particle exchange. Geometrically a two-particle exchange is more seriously affected than the higher order ones, resulting in the effective FM behavior in the  $R$  phase. Of course, an exact calculation of  $J_n$  by path integral Monte Carlo techniques would be required to make a quantitative discussion. Another explanation is also possible. Such a low density solid may contain zero point vacancies which would polarize the surrounding spins. However, the situation is somewhat complicated for the nonalternate triangular lattice. Theory predicts the ground state may not be ferromagnetic [22,23]. In addition to the magnetic behavior, the specific heat in the  $R$  phase has a strange  $T^{-1}$  dependence over the wide temperature region [12,24]. Since its origin has not yet been clarified, it is desirable to develop a theory consistent with both magnetic and thermodynamic properties.

In conclusion, we have made, for the first time, NMR measurements of the first layer solid  $^3\text{He}$  on graphite down to  $120 \mu\text{K}$ . The antiferromagnetic behavior is observed just between the ferromagnetic incommensurate and the  $\sqrt{3} \times \sqrt{3}$  commensurate phases. Variation from AFM to FM with increasing the areal density is very similar to that of the second layer, and can be explained by the

competition of the in-plane multiple spin exchanges. This fact gives a strong evidence that the ferromagnetic behavior in the second layer comes from in-plane exchange processes. However, the cause of the ferromagnetism observed for the  $\sqrt{3} \times \sqrt{3}$  phase still remains unclear. Further theoretical investigation for MSE including the effect of corrugation potential is eagerly desired.

We thank Professor Hiroshi Fukuyama for valuable discussions.

- 
- [1] M. Roger, J.H. Hetherington, and J.M. Delrieu, *Rev. Mod. Phys.* **55**, 1 (1983).
- [2] M. Roger, C. Bäuerle, Yu.M. Bunkov, A.-S. Chen, and H. Godfrin, *Phys. Rev. Lett.* **80**, 1308 (1998); M. Siqueira, J. Nyéki, B. Cowan, and J. Saunders, *Phys. Rev. Lett.* **78**, 2600 (1997).
- [3] H. Godfrin and R.E. Rapp, *Adv. Phys.* **44**, 113 (1995).
- [4] M. Roger, *Phys. Rev. Lett.* **64**, 297 (1990); *Phys. Rev. B* **30**, 6432 (1984).
- [5] S. Tasaki, *Prog. Theor. Phys.* **81**, 946 (1989).
- [6] R. A. Guyer, *Phys. Rev. Lett.* **64**, 1919 (1990).
- [7] H. Godfrin, R.E. Rapp, K.-D. Morhard, J. Bossy, and C. Bäuerle, *Phys. Rev. B* **49**, 12 377 (1994).
- [8] J. Saunders, C.P. Lusher, and B.P. Cowan, *Phys. Rev. Lett.* **64**, 2523 (1990); M. Siqueira, C. Lusher, B. Cowan, and J. Saunders, *J. Low Temp. Phys.* **89**, 619 (1992).
- [9] R.E. Rapp and H. Godfrin, *Phys. Rev. B* **47**, 12 004 (1993).
- [10] Grafoil is exfoliated graphite manufactured by Union Carbide.
- [11] H. Ishimoto, H. Fukuyama, T. Fukuda, T. Okamoto, T. Tazaki, K. Sakayori, and S. Ogawa, in *Quantum Fluids and Solids—1989*, edited by G.G. Ihas and Y. Takano, AIP Conf. Proc. No. 194 (AIP, New York, 1989), p. 281.
- [12] D.S. Greywall and P.A. Busch, *Phys. Rev. Lett.* **65**, 2788 (1990).
- [13] D.S. Greywall and P.A. Busch, *Phys. Rev. Lett.* **65**, 64 (1990).
- [14] B. Bernu, D. Ceperley, and C. Lhuillier, *J. Low Temp. Phys.* **89**, 589 (1992).
- [15] D.S. Greywall, *Phys. Rev. B* **41**, 1842 (1990).
- [16] B. Cowan, L.A. El-Nasr, M. Fardis, and A. Hussain, *Phys. Rev. Lett.* **58**, 2308 (1987).
- [17] H. Franco, R.E. Rapp, and H. Godfrin, *Phys. Rev. Lett.* **57**, 1161 (1986).
- [18] P. Schiffer, M.T. O’Keefe, D.D. Osheroff, and H. Fukuyama, *Phys. Rev. Lett.* **71**, 1403 (1993).
- [19] M. Siqueira, J. Nyéki, B. Cowan, and J. Saunders, *Czech. J. Phys. Suppl. S6* **46**, 3033 (1996).
- [20] M. Siqueira, C.P. Lusher, B.P. Cowan, and J. Saunders, *Phys. Rev. Lett.* **71**, 1407 (1993).
- [21] M.W. Cole, D.R. Frankl, and D.L. Goodstein, *Rev. Mod. Phys.* **53**, 199 (1981).
- [22] M. Héritier and P. Lederer, *Phys. Rev. Lett.* **42**, 1068 (1979).
- [23] K. Machida and M. Fujita, *Phys. Rev. B* **42**, 2673 (1990).
- [24] M. Morishita, H. Nagatani, and Hiroshi Fukuyama, *J. Low Temp. Phys.* (to be published).